Proceedings of the 29th Annual International
Conference of the IEEE EMBS
Cité Internationale, Lyon, France
August 23-26, 2007.

Action Potential Alternans in LQT3 Syndrome: A Simulation Study

Felipe Alonso-Atienza, Jesús Requena-Carrión, José Luis Rojo-Álvarez,
Omer Berenfeld and José Jalife

Abstract— **The long QT syndrome type-3 (LQT3) is an inherited cardiac disorder caused by mutations in the sodium channel gene SCN5A. LQT3 has been associated with ventricular arrhythmias and sudden cardiac death, specially at low heart rates. Based on computer simulations and experimental investigations, analysis of the morphology of the Action Potential (AP) has shown that it undergoes early afterdepolarizations (EADs) and spontaneous discharges, which are thought to be the trigger for reentry like-activity. However, dynamic characteristics of cardiac tissue are also important factors of arrhythmia mechanisms. In this work, we propose a dynamical analysis of the LQT3 at cellular level. We use a detailed Markovian model of the ΔKPQ mutation, which is associated with LQT3, and we study beat-to-beat AP Duration (APD) variations by using a long-term stimulation protocol. Compared to wild-type (WT) cells, ΔKPQ mutant cells are found to develop APD alternans over a narrow range of stimulation frequencies. Moreover, the interval of frequency dependence of APD alternans is related to the degree of severity of the EADs present in the AP. In conclusion, dynamical analysis of paced cells is a useful approach to understand the mechanisms of rate dependent arrhythmias.**

I. INTRODUCTION

The long QT syndrome type-3 (LQT3) is an inherited cardiac disease characterized by a delayed ventricular repolarization that manifests as prolongation of the QT segment in the electrocardiogram (ECG). LQT3 has been associated with complex ventricular arrhythmias and ventricular fibrillation (VF), preferentially at low heart rates, during rest or sleep periods [1]. LQT3 is caused by mutations in the cardiac sodium channel gene SCN5A. Deletion of the amino acids KPQ (ΔKPQ) in SCN5A is one of the most severe mutations associated with the LQT3, as it disrupts the inactivation process [2]. Mutant channels continue to reopen at depolarized membrane potentials, hence inducing a small persistent inward current which prolongs the action potential duration (APD) and leads to a QT lengthening [2], [3]. Prolongation of the APD, as well as the presence of early afterdepolarizations (EADs) has been confirmed in in-vitro experiments in ΔKPQ transgenic mice [4], [5]. EADs are thought to be the trigger of cardiac arrhythmia in the settings of LQT3, however, the mechanisms by which they promote an arrhythmogenic behavior are not fully understood.

Complementary to in-vitro experiments, computer models have been also used to understand the mechanisms of cardiac arrhythmia in the LQT3 syndrome. Clancy and Rudy developed a cellular AP model of the ΔKPQ, by means of a Markovian description of the wild-type (WT) and ΔKPQ mutant (MT) channels [6]. Their results showed bradycardia-dependent delayed repolarization that may lead to EADs. Based on an analysis of the AP morphology, this model has been used to link genetic cardiac mutations to its cellular manifestation [7], [8], and to evaluate the effects of drug therapy to manage cardiac arrhythmias [9]. However, besides anomalies in the AP morphology due to EADs, abnormal beat-to-beat phenomena, like APD alternans, are important factors and predictors of cardiac arrhythmia [10]. Therefore, the aim of this study is to analyze with detail the beat-to-beat variations of the ΔKPQ-LQT3 model. We characterize dynamically both the WT and the ΔKPQ MT cells by a long-term stimulation protocol. Simulations show that MT cell exhibit APD alternans. Furthermore, these APD alternans are found at stimulation frequencies where intermittent EADs are present, thus generating unstable beat-to-beat AP changes.

In the following sections, we first introduce the computer model and stimulation protocol. Secondly, we investigate the dynamic properties of the LQT3-ΔKPQ model and we present our main results. Thirdly, we discuss the principal findings. Finally, we summarize our results and propose future research.

II. METHODS

A. Single Cell Model

Single cell behavior was simulated by using the Luo-Rudy model (LRd) of the ventricular AP for the guinea pig [11]. The AP is reconstructed according to the following differential equation:

$$\frac{dV_m}{dt} = -\frac{1}{C_m} \cdot (I_{ion} + I_{st}) \qquad (1)$$

which relates the rate of change of the transmembrane potential (V_m) to the total ionic transmembrane currents (I_{ion}) and the stimulation current (I_{st}). C_m represents the membrane capacitance and is set to 1 $\mu F/cm^2$. The LRd computes the AP from voltage-gated ionic channels, pumps, and exchangers. The model also accounts for processes that regulate intracellular concentration changes of sodium

This work was been partially supported by Research Grant from Guidant Spain to J.L. Rojo-Álvarez, and by grants PO1 HL039707, RO1 HL070074, and RO1 HL080159 from the USA National Institutes of Health to J. Jalife. J. Requena-Carrión is supported by Grant 01-836-04 from Consejería de Educación de la Comunidad de Madrid.

F. Alonso-Atienza, J. Requena-Carrión and J.L. Rojo-Álvarez are with Department of Signal Theory and Communications, Universidad Rey Juan Carlos, Camino del Molino s/n, 28943 Fuenlabrada, Madrid, Spain falonso@tsc.uc3m.es, jesus@tsc.uc3m.es, joseluis.rojo@urjc.es

O. Berenfeld and J. Jalife are with Department of Pharmacology, Institute of Cardiovascular Research, Upstate Medical University of New York, 766 Irving Avenue, Syracuse, NY 13210, USA berenfeo@upsate.edu, jalifej@upstate.edu

(Na^+), potassium (K^+), and calcium (Ca^{2+}) ions. All the ionic currents, except for the fast sodium current (I_{Na}), are formulated according to the Hodgkin-Huxley formalism. A detailed description of each current can be found in the original paper [11].

B. Markovian Model of the I_{Na}

The gating behavior of the sodium channel is represented as a continuos-time Markov model. This Markovian representation of the I_{Na} is integrated into the single cell model, yielding a computer model that simulates the ΔKPQ mutation associated with the LQT3 syndrome (see [9] for more details). The ΔKPQ-LQT3 model accounts for both WT and ΔKPQ channels, so the total output macroscopic sodium current can be expressed as

$$I_{Na} = \alpha \cdot I_{Na-MT} + (1-\alpha) \cdot I_{Na-WT} \qquad (2)$$

where I_{Na-MT} is the current produced by MT channels, I_{Na-WT} the current produced by WT channels, and α is the *penetrance index*, i.e. the proportion of WT and MT channels, in such a way that:

- $\alpha = 0$ represents a WT cell;
- $\alpha = 0.5$ represents a heterozygous cell;
- $\alpha = 1$ represents a homozygous MT cell.

The accuracy of this model has been thoroughly tested and validated according to experimental data [6]–[9].

C. Simulation conditions

All simulations were performed on a desktop PC (3GHz, 2GB RAM), using C/C++. The integration time step was taken to be $\Delta t = 0.005$ ms. The APD is defined as the interval between the AP upstroke and the repolarization potential of -70 mV, which is approximately the APD at 90% repolarization.

D. Stimulation protocol

In this paper, beat-to-beat APD variations are characterized by using a long-term stimulation protocol. Starting from an initial Basic Cycle Length (BCL) B_0, both WT and ΔKPQ cells are paced at decreasing BCLs (B). For each cycle length B, cells are stimulated for 60 seconds. After that, B is decreased in Δ ms, so $B_{new} = B_{old} - \Delta$. The protocol is repeated until the minimum value of B for which an APD can be elicited for each given stimulus is attained. By means of this protocol, the temporal evolution of the APD can be obtained (Fig. 1). This is a useful representation, since it shows how the APD *accommodates* [12] in response to step decrements in B. Abrupt changes in the APD result at time instants where decrements in B take place (vertical dotted lines). Then, as time goes by, the APD slowly reaches the steady-state, until another stimulation rate is used.

III. Results

A. Stimulation protocol of the WT

Fig. 1 illustrates the results of applying the stimulation protocol to a WT cell. As the value of B was changed, the WT cell responded in a stable 1:1 manner. This response pattern corresponds to a normal behavior, in which APD variations from one beat to the other are negligible (for the same B).

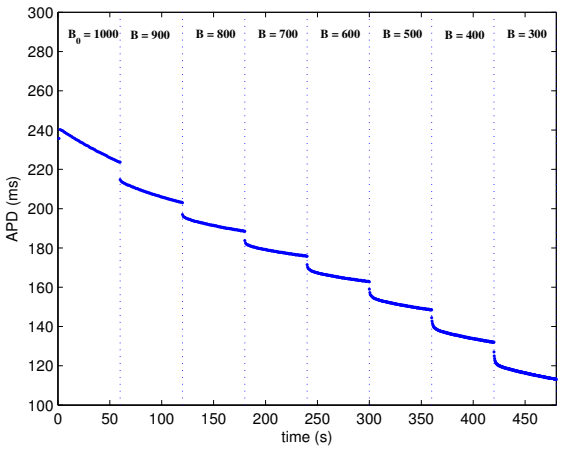

Fig. 1. Stimulation protocol for a WT cell. From a starting value of $B_0 = 1000$ ms, cycle length was decreased until $B = 300$ ms, with $\Delta = 100$ ms. For each B, the APD slowly reaches the steady-state (APD accommodation). Even if the APD seems not to reach a steady-state, longer stimulation periods -i.e. 120 s- has been studied showing that effectively it does.

B. Stimulation protocol of the MT

A very different behavior results when applying the stimulation protocol to a ΔKPQ MT cell. The APD accommodation of a heterozygous cell ($\alpha = 0.5$) is plotted in Fig. 2 (a). As shown, for $B = 800$ and 700 ms, the APD does not have a steady-state, rather it alternates between a discrete set of values. Thus, the APD oscillates from one of these values to the other on a beat-to-beat basis. An example of the beat-to-beat variation of the AP can be seen in Fig. 2 (b). Unstable EADs disrupt the balance between the APD and the preceding diastolic interval (DI). In consequence, the APD never reaches a steady state, giving rise to APD alternans. Pacing cycle intervals B, for which no EADs ($B = 600$ to 300 ms), or stable EADs ($B = 1000$ and 900 ms) are present, do not show APD alternans (Fig. 3).

In a homozygous ΔKPQ cell ($\alpha = 1.0$), APD alternans arises over a wider range of stimulation intervals when compared to a heterozygous cell (Fig. 4 (a)). In this case, there are no stable states until the 1:1 response returns at $B = 300$ ms. It is also remarkable that the AP shows large EADs, thus indicating that the larger the EADs, the more unstable the APD.

We have found that the results presented above are not dependent on the values of B_0 and Δ. Test values of B_0 ranged between $B_0 \pm 200$ ms of the original value (i.e B_0 = 1000 for heterozygous cell). Δ has been changed from small values ($\Delta = 10$ ms), to larger values ($\Delta = 500$ ms). Simultaneous variations of both B_0 and Δ also yielded similar results.

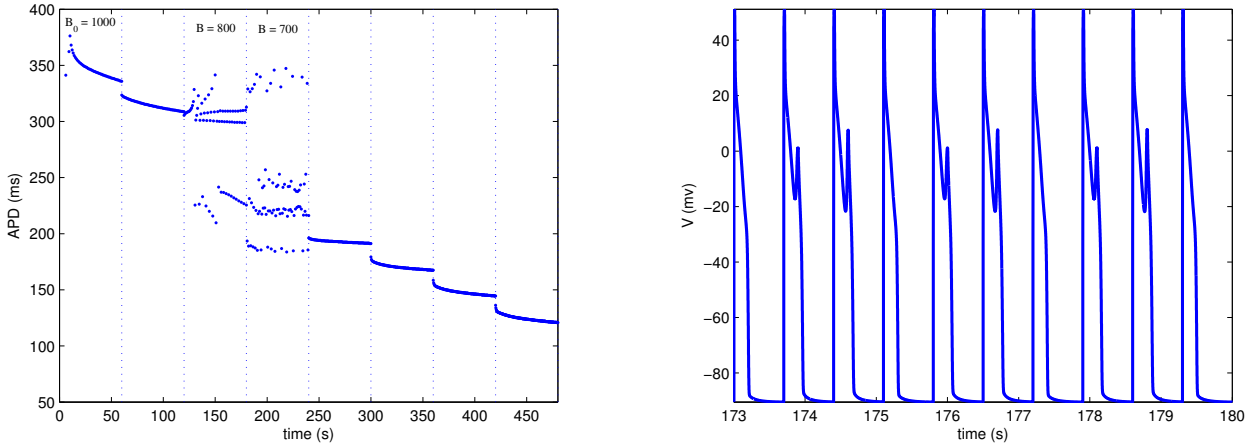

(a) (b)

Fig. 2. Stimulation protocol applied to a heterozygous cell. (a) APD accommodation; simulations parameters are the same as for the WT ($B_0 = 1000$ ms, $\Delta = 100$ ms). (b) A sequence of APs exhibiting APD alternans. This behavior corresponds to APs measured at $B = 800$ ms.

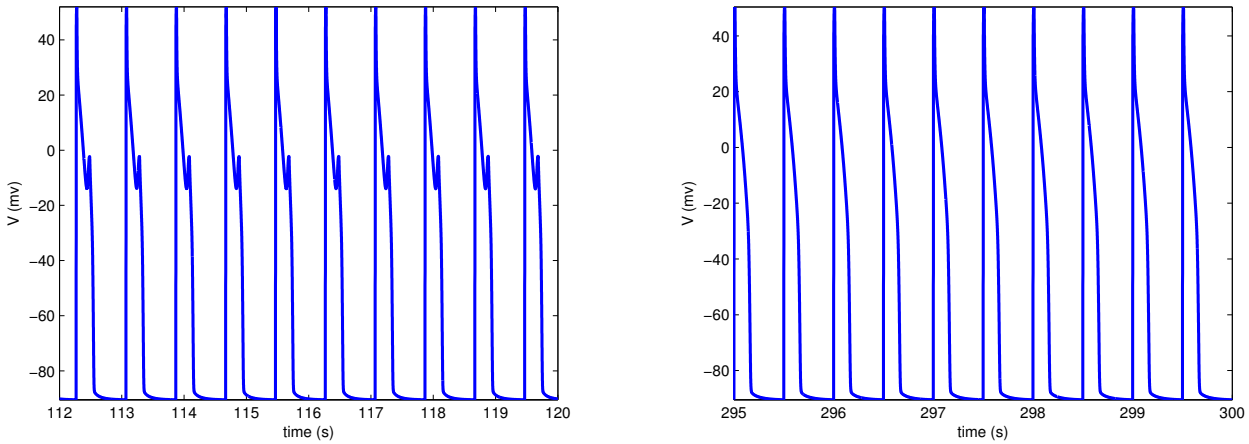

(a) (b)

Fig. 3. Sequences of APs of a heterozygous cell measured at different time instants. (a) Before APD alternans occur ($B = 900$ ms). (b) After APD alternans take place ($B = 600$ ms).

IV. DISCUSSION

In the present study, we have analyzed the dynamic behavior of both WT and ΔKPQ cells, using a Markovian computer model of the ΔKPQ-LQT3 syndrome subjected to a long-term stimulation protocol. A picture of the time evolution of the APD identified APD alternans in MT cells over a narrow range of stimulation frequencies. This result may help to explain why patients with ΔKPQ mutation are likely to develop arrhythmias within different heart rate ranges compared with normals or other types of LQT syndrome [1]. More interestingly, APD alternans is also linked to T waves alternans [13], an ECG phenomenon associated with LQT syndrome that has been proposed as an important harbinger for ventricular arrhythmia [14]. On the other hand, presence of EADs is not a sufficient condition to generate alternans, as for very low stimulation intervals (i.e. $B > 900$ ms for a heterozygous cell) APs with stable EADs do not show APD alternans. However, in a narrow band of stimulation intervals, EADs generated in MT cells induce irregularities in the DI, leading to beat-to-beat irregularities in the APD. Further, as it was shown when comparing heterozygous and homozygous MT cells, large EADs produces irregularities (alternans) at the APD in wider range of stimulation frequencies.

V. CONCLUSIONS AND FUTURE WORK

Our simulations demonstrate that a dynamical analysis at the cellular level based on computer simulations is an useful approach to link molecular defects to mechanisms of rate dependent arrhythmias. We have also shown that potential mechanisms of LQT3 arrhythmias can not be attributed exclusively to EADs or APD alternans, but to a contribution of both factors. Future research should study the dynamic dependence between EADs and APD alternans. Extensions of the cellular model proposed here, to one-dimensional and two-dimensional ventricular tissue models,

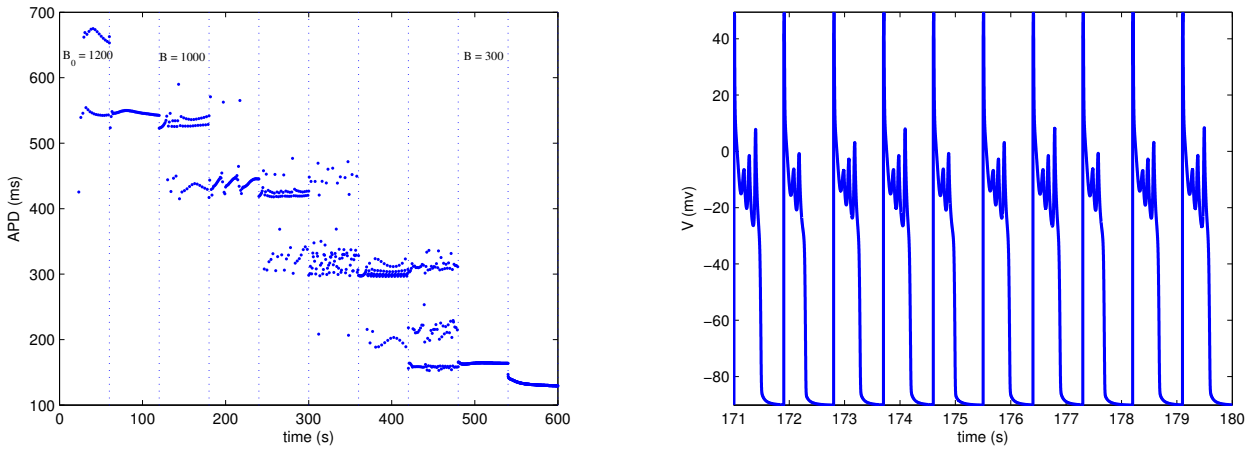

(a) (b)

Fig. 4. Stimulation protocol applied to a homozygous MT cell. (a) APD accommodation, simulations were carried out for $B_0 = 1200$ ms and $\Delta = 100$ ms. (b) A sequence of APs exhibiting APD alternans. This behavior corresponds to APs measured at $B = 1000$ ms.

would allow us to analyze further the mechanism of cardiac arrhythmia in terms of both EADs and spatially discordant APD alternans [15]. Finally, the predictions of this theoretical analysis based on computer simulations are readily testable in experiments using cardiac cells that express the ΔKPQ and other mutations that are relevant to the LQT syndrome.

VI. ACKNOWLEDGMENTS

We thank Drs. Colleen E. Clancy and Zheng I. Zhu for providing source code used in this study and for kind technical support.

REFERENCES

[1] P. J. Schawrtz, "The congenital long QT syndromes from genotype to phenotype: clinical implications," *J. Intern. Med.*, vol. 259, no. 1, pp. 39–47, Jan 2006.

[2] R. Dumaine, Q. Wang, M. T. Keating, H. A. H. andP. J. Schwartz, A. M. Brown, and G. E. Kirsch, "Multiple mechanisms of na+ channel–linked long-qt syndrome," *Circ. Res.*, vol. 78, no. 5, pp. 916–924, May 1996.

[3] R. Chandra, C. F. Starmer, and A. O. Grant, "Multiple effects of KPQ deletion mutation on gating of human cardiac na+ channels expressed in mammalian cells," *Am. J. Physiol.*, vol. 274, no. 5, pp. H1643–54, May 1998.

[4] D. N. D, M. Stengl, S. Dugarmaa, T. Rossenbacker, V. Compernolle, Y. Rudy, J. F. Smits, W. Flameng, C. E. Clancy, L. Moons, M. A. Vos, M. Dewerchin, K. Benndorf, D. Collen, E. Carmeliet, and P. Carmeliet, "Abrupt rate accelerations or premature beats cause life-threatening arrhythmias in mice with long-qt3 syndrome," *Nat. Med.*, vol. 7, no. 9, pp. 1021–7, Sep. 2001.

[5] C. E. Head, R. Balasubramaniam, G. Thomas, C. A. Goddard, M. Lei, W. H. Colledge, A. A. Grace, and C. L. Huang, "Paced electrogram fractionation analysis of arrhythmogenic tendency in deltakpq scn5a mice," *J. Cardiovasc. Electrophysiol.*, vol. 16, no. 12, pp. 1329–1340, Dec. 2005.

[6] C. E. Clancy and Y. Rudy, "Linking a genetic defect to its cellular phenotype in a cardiac arrhythmia," *Nature*, no. 400, pp. 566–569, Aug. 1999.

[7] C. E. Clancy, M. Tateyama, and R. S. Kass, "Insights into the molecular mechanisms of bradycardia-triggered arrhythmias in long QT-3 syndrome," *J. Clin. Invest.*, vol. 110, no. 9, pp. 1251–62, Nov. 2002.

[8] C. E. Clancy and Y. Rudy, "Na(+) channel mutation that causes both brugada and long-QT syndrome phenotypes: a simulation study of mechanism," *Circulation*, vol. 105, no. 10, pp. 1208–13, Mar. 2002.

[9] C. E. Clancy, Z. I. Zhu, and Y. Rudy, "Pharmacogenetics and anti-arrhythmic drug therapy: a theoretical investigation," *Am. J. Physiol. Heart. Circ. Physiol.*, vol. 292, no. 1, pp. 66–75, Jan. 2007.

[10] J. N. Weiss, A. Karma, Y. Shiferaw, P. S. Chen, A. Garfinkel, and Z. Qu, "From pulsus to pulseless: the saga of cardiac alternans." *Circ. Res.*, vol. 98, no. 10, pp. 1244–53, May. 2006.

[11] C. H. Luo and Y. Rudy, "A dynamic model of the cardiac action potential. ii. afterdepolarizations, triggered activity, and potentiation." *Circ. Res.*, vol. 74, no. 6, pp. 1097–113, Jun. 1994.

[12] M. A. Watanabe and M. L. Koller, "Mathematical analysis of dynamics of cardiac memory and accommodation: Theory and experiments," *Am. J. Physiol. Heart Circ. Physiol.*, vol. 282, no. 4, pp. H1534–47, Apr. 2002.

[13] J. M. Pastore, S. D. Girouard, K. R. Laurita, F. G. Akar, and D. V. Rosenbaum, "Mechanism linking T-wave alternans to the genesis of cardiac fibrillation." *Circulation*, vol. 99, no. 10, pp. 1385–94, Mar. 1999.

[14] J. M. Pastore, K. R. Laurita, and D. V. Rosenbaum, "Importance of spatiotemporal heterogeneity of cellular restitution in mechanism of arrhythmogenic discordant alternans." *HeartRhythm*, vol. 3, no. 6, pp. 711–9, Jun. 2006.

[15] H. Hayashi, Y. Shiferaw, D. Sato, M. Nihei, S. F. Lin, P. S. Chen, A. Garfinkel, J. N. Weiss, and Z. Qu, "Dynamic origin of spatially discordant alternans in cardiac tissue," *Ann. N. Y. Acad. Sci.*, vol. 92, no. 2, pp. 448–60, Jan. 2007.